Kevin W. Reynolds is a junior at Norfolk State University where he is pursuing a BS in physics with a minor in mathematics. Reynolds worked at Stanford Linear Accelerator Center where he tested high-resolution silicon and germanium analyzers to be used in a X-Ray Raman Spectrometer for probing the fundamental structure of liquid water. At the conclusion of his research, he was awarded the Ernest Coleman Award by SLAC for outstanding initiative and citizenship as a young researcher. Kevin presented at the 2005 Annual AAAS meeting and was recognized as a winner of the Physical Science poster session. This coming summer he plans to do an internship through the MURF program at Caltech where he will build microfluidic channels with possible medical application. Reynolds plans to attend graduate school in aerospace engineering.

Uwe Bergmann is a Staff Scientist at the Stanford Synchotron Radiation Laboratory which is part of the Stanford Linear Accelerator Center. He received his Ph.D. in Physics from Stony Brook University, NY in 1994. Following a 2-year postdoc at the European Synchrotron Radiation Facility in Grenoble, France he joined Lawrence Berkeley National Laboratory (LBNL), first as a postdoc then as a scientist. Before joining SSRL in 2003 he held a joint appointment LBNL and University of California, Davis. His current research interests include the development and application of novel x-ray spectroscopic techniques to study transition metal complexes and low Z materials including water. The particular techniques are non-resonant x-ray Raman scattering, resonant inelastic x-ray scattering, x-ray emission spectroscopy and selective x-ray absorption spectroscopy. Most recently he has started work on x-ray fluorescence imaging of the Archimedes Palimpsest.

TESTING OF HIGH-RESOLUTION SI AND GE ANALYZERS FOR X-RAY RAMAN SCATTERING AND X-RAY EMISSION SPECTROSCOPY

KEVIN W. REYNOLDS, UWE BERGMANN

ABSTRACT

A project at Stanford Linear Accelerator Center (SLAC) is currently underway for the building of a new multi-crystal x-ray spectrometer that will be used to probe the fundamental structures of light elements, including water, as well as 3d transition metals, such as metalloproteins, in dilute systems. Experimentation for determining the focal lengths for the prospective high-resolution, spherically-curved silicon (Si) and germanium (Ge) analyzers for the instrument and the energy resolutions at their respective focal points is described. The focal lengths of the Si and Ge analyzers being sampled were found by minimizing the focal size made from a diffused helium-neon (HeNe) gas laser operating at 632 nm (0.95 meV). Afterwards, the energy resolutions were determined by using synchrotron radiation (SR), in the range from 6-16 keV energies. The experiments were performed at Beamline 10-2 at the Stanford Synchrotron Radiation Laboratory (SSRL), a division of SLAC. This data, along with the energies of the incident beams, was used to determine which samples are most effective at focusing x-rays to the highest spatial and energy resolution. Sample Si (440)A, with a focal length of 1015.2 mm, had the best energy resolution. Furthermore, a new multi-crystal goniometer was tested and commissioned. As part of this work, the device was prealigned into Rowland geometry, in order to facilitate the process of finding a single high-energy resolution x-ray focus for all 7 analyzers.

INTRODUCTION

As strange as it may seem, water, taken to be one of nature's most fundamental elements, has been and still is, in large part, a mystery. For the past 20 years, scientists have maintained a consensus that a typical water molecule forms, on average, 3.5 hydrogen bonds with nearby water molecules at any moment in time. But recent research, based partly on X-ray Raman scattering (XRS), suggests that there might be only two hydrogen bonds per molecule [1-3]. The confirmation of such an assignment would have dramatic consequences in the whole field of water research. Therefore efforts are under way to build a new, more efficient, instrument for future X-ray Raman studies. The device will also be used for other studies including X-ray Emission spectroscopy (XES) on 3d transition metals.

In prototyping for a new instrument, several innovations will be made and compared to a previous design [4]. An essential requirement for the instrument is the ability to diffract one particular energy back to a focal point in order to obtain information about the scattered/emitted x-ray energy. At the same time, a large solid angle should be captured to make the measurement efficient. Bragg diffraction, as used in this paper, underlies the mechanism of how the instrument works. Each analyzer needs to be capable of good energy resolution and large angular acceptance. To achieve the highest energy resolution and smallest focus possible, a variety of

Si and Ge crystals are tested. In order to characterize analyzers appropriately both the focal sizes and energy resolution spectra are measured and compared. The first experimental setup uses a HeNe gas laser to measure the respective focal lengths and focal sizes of the analyzers. The second arrangement incorporates the found values by using synchrotron radiation to study the energy resolutions found at those lengths. In this report, we show which crystals will provide the best resolution for the new X-ray spectrometer. This data has been used to determine from which provider the analyzer crystals for the new instrument will be purchased.

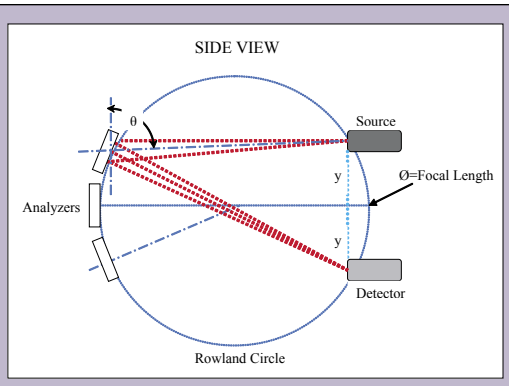

Figure 1. Left: Side view of a Rowland Geometry that shows how a diffused radiation source is focused back to a detector through elastic scattering at a Bragg angle θ. Right: Photo of Experiment I setup showing the superimposed path of the diffused laser as it hits the analyzer.

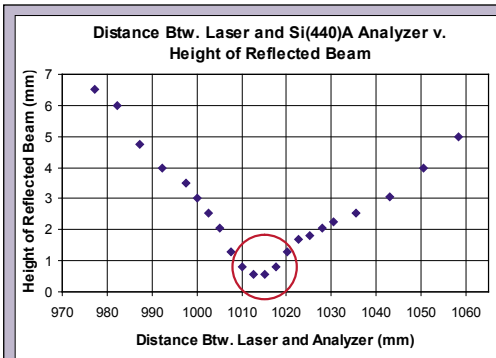

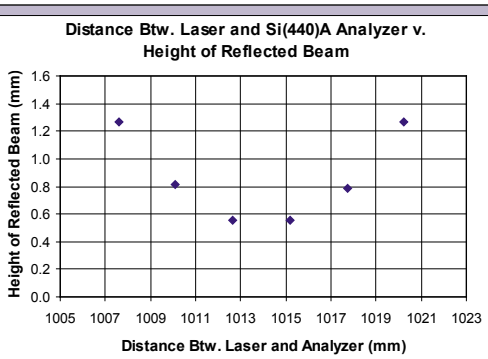

Figure 2. *Left:* Graph showing relationship between distance and height of beam. *Right:* Graph showing magnified view of the region containing the focus.

MATERIALS AND METHODS

Bragg's Law

To effectively monochromatize, or make of a single frequency, radiation being scattered from a point source, a special geometry, called Rowland geometry, serves as a means for capturing a large portion of the solid angle of scattered light without significant energy resolution loss. Still, even in Rowland geometry the energy resolution is limited, mainly due to stresses in the crystal structure, geometric effects related to the beam size, and non-perfect spherical bending of the silicon and germanium wafers into the concavity of each different analyzer. When collimated x-rays hit a crystalline solid, their approximately energy upon reflection can be obtained from Bragg's Law,

$$2\,d \sin\theta = n\,\lambda, \qquad (1)$$

where θ is the Bragg angle or angle of incidence, λ is the wavelength of the incident x-rays, *n* is an integer describing multiples of the wavelength, and *d* is the spacing between sequentially planes in the crystal [5, 6]. The distance $d = a / (h^2 + k^2 + l^2)^{1/2}$, where *a* is the lattice parameter and *h*, *k*, and *l* are Miller indices, or coordinates defining the orientation of the intrinsic crystalline planes. Since the *d*-spacing is extraordinarily minute, monochromators often are used to make beams having energies well above 1 keV uniform in wavelength. The inverse relationship between wavelength λ and energy *E* is shown by

$$E = \hbar c / \lambda \quad \rightarrow \quad E[\text{keV}] = 12.3985 / \lambda[\text{Å}] \qquad (2)$$

with wavelength being given in Å and energy being obtained in keV. As can be drawn from Eq. 1, the wavelength of the incident beam has to be less than two times the distance between sequential planes in the crystal in order for the wave to be diffracted.

To estimate the energy resolution of Bragg optics, we form the derivative of Eq. 1 shown by

$$|\Delta E/E| = |\Delta\lambda / \lambda| = \Delta\theta \cot\theta. \qquad (3)$$

Equation 3 shows that for a given angular spread Δθ, the smallest energy resolution $\Delta E/E$ can be achieved at Bragg angles close to 90° where *cot* θ becomes very small. This is why high-energy resolution Bragg optics is operated in back scattering, where θ is close to 90°.

Rowland's Geometry

Focusing of a radiation source can be achieved by either employing a spherical arrangement of a large number of small flat crystals, which ultimately results in the best focus, or by bending Miller planes in the structure of a single crystal. Our instrument utilizes a unique combination of the two; it calls for eventually positioning 28 spherically-curved crystals on intersecting Rowland circles with a diameter equal to the established focal length (Figure 1). This compromise of energy resolution and capturing of a large solid angle of the scattered radiation has become a promising means of obtaining an efficient analyzer. In Rowland geometry, analyzers source and detector are positioned on a circle (Rowland circle), with both source and detector at a distance *y* above and below the diameter (see Figure 1) [4]. Once completed, the analyzer system should capture ~1.75 % of the total 4π solid angle, a factor 4 improvement over the previous x-ray spectrometer [4]. By covering

greater portions of the solid angle, higher efficiency can be achieved for examining unsolved aspects of the light elements and 3d transition metals.

Experiment I

In order to characterize the eight different analyzers for the highest energy resolution, the focal length of each of the analyzers was experimentally determined. The crystals ranged from thicknesses of 0.15 to 0.5 mm. They were glued or ionically bonded on spherically-curved glass substrates with radii of curvature ranging from 850 to 1020 mm. The diameters of the substrates ranged from 90 mm to 100 mm.

The focal length of each of the analyzers was found using a HeNe laser diffused radially by a simple scatterer, a piece of clear tape, placed overtop of the front lens. One at a time, each analyzer was fastened into a metal frame holder mounted vertically on a manually-operated, screw-transitioned table. The distances traveled closer to and farther away from the laser source were recorded in increments of 2.54 mm. This distance was the calculated horizontal distance traveled during one revolution of the turning screw. The analyzer was positioned 5 mm vertically below the laser's focal point to fulfill the Rowland condition (see again Figure 1) so that the reflected laser beam appeared 10 mm below the laser source on a white piece of paper attached to the front of the encasement for the laser.

The height of the focus was measured using a micro telescope, leveled off at horizontal, which assigned number values on a scale of 0.01 of an inch, to the vertical extremes of the diffracted beam. These numbers were added, divided by 1000, and multiplied by 25.4 to find the height of the beam in millimeters. Heights larger than 4.5 mm were measured with a ruler. Graphs were produced for all of the analyzers and related the horizontal distance between the laser and analyzer and the size of the diffracted beam as shown in Figure 2. The region surrounding the minimum of the graph was magnified and used to identify a minimum focal size. The distance corresponding to the focal size was recorded.

Since these measurements only accounted for the horizontal distance R to the outer edges of the analyzer, the focal length F was calculated using a right triangle diagram as shown in Figure 3. Later, the concavity Δx was determined by subtracting distance R from distance F.

Experiment Ii

At SSRL, electrons are accelerated in a circular vacuum loop, known as booster, to nearly the speed of light were they form packets of electrons known as bunches. These bunches are approximately the diameter of a human hair. From the synchrotron, the bunches are then fed into a storage ring where bending magnets change the direction of the beam at twelve different locations. At these selected turns, the fast-moving electrons lose some of their energy in the form of emitted photons, or electromagnetic radiation known as synchrotron radiation. In addition, to these bending magnets SSRL also employs arrays of magnets known as wigglers. Because the electrons undergo multiple lateral accelerations these wigglers produce even more intense synchrotron radiation. The electrons continue through the storage ring where electromagnetic kickers replenish their lost energy so a constant energy can be maintained. The radiation emitted by the electron bunches produces a broad spectrum of synchrotron light ranging from infrared to x-rays. Conveniently, tangential ports channel the radiation into beamlines which end at experimental stations. Horizontal and vertical focusing mirrors increase the spatial resolution of the beam. A monochromator selects a specific wavelength, and thus a specific energy. In our experiments, the slit width in front of the scatterer was set to 0.12 mm horizontal X 1.00 mm vertical.

Experiment II used synchrotron radiation to identify the highest energy resolutions produced by the analyzers at their measured focal lengths. Upon entering the experimental hutch, or end station, at wiggler Beamline 10-2, the x-rays were directed through an ion chamber filled with nitrogen gas. As the x-rays passed through the chamber, they knocked

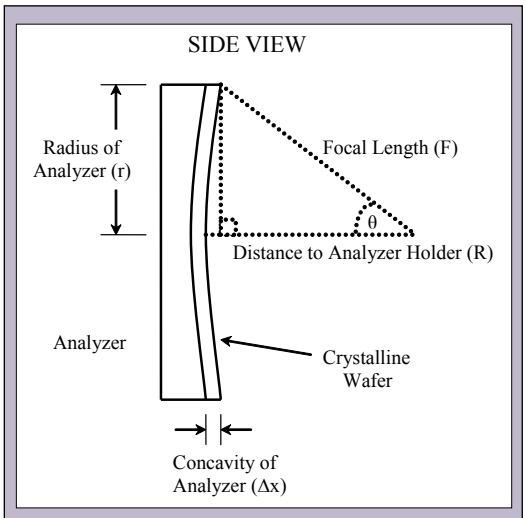

Figure 3. Detailed side view schematic for calculating the focal length F of an analyzer and determining its concavity x. As noted in *Fig.1 Left*, the distance R on the Rowland circle is half of the focal length.

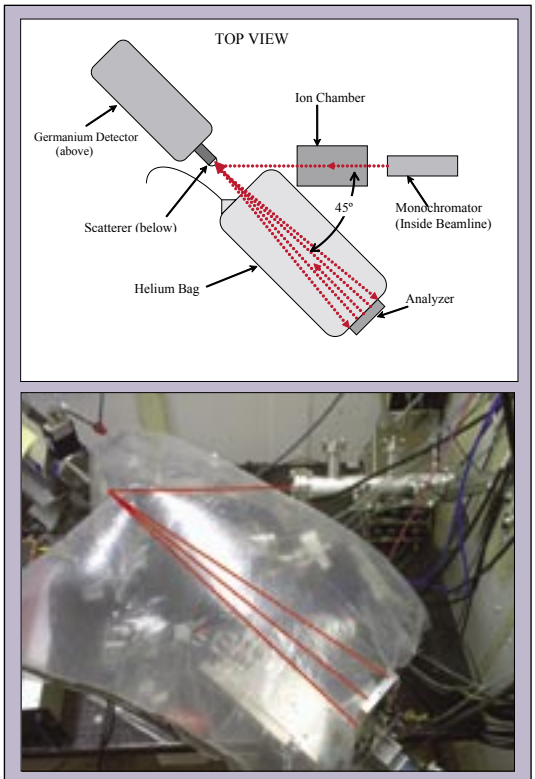

Figure 4. *Above* Top view of the schematic setup for Experiment II demonstrating the 45˚ chosen for back scattering. *Below:* Photo showing Experiment II setup and a superimposed path of the invisible synchrotron radiation as it hits the analyzer.

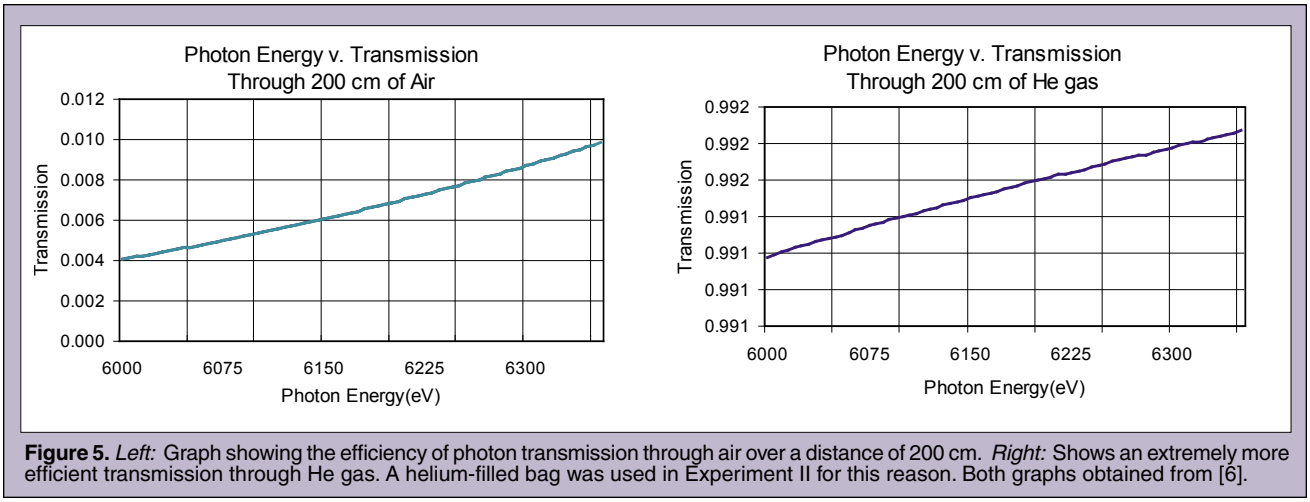

Figure 5. *Left:* Graph showing the efficiency of photon transmission through air over a distance of 200 cm. *Right:* Shows an extremely more efficient transmission through He gas. A helium-filled bag was used in Experiment II for this reason. Both graphs obtained from [6].

electrons out of the nitrogen atoms and produced a cloud of free electrons. A high voltage across two plates inside of the chamber pulled away the electrons to a positively charged anode. In turn, the measured current was proportional to the intensity of the x-rays passing through the chamber.

After passing through the ion chamber, the beam was scattered by a piece of paraffin taped to a metal column. The instrument holding the analyzer was placed at a 45˚angle adjacent to the incoming x-ray (see Figure 4). For purposes of limiting the attenuation of x-rays from air, a plastic bag was filled with helium gas and placed between the scatterer and analyzer. The difference in the absorption of photons as they propagate through the two gases is depicted in the graphs contained in Figure 5. According to the figures, transmission of 6.46 keV x-rays through helium gas is about 100 times in magnitude better than transmission through air over the same 200 cm distance. In fact, the transmission through the helium gas is nearly 100%, and loss in the plastic of the bag is also negligible. This compliment to our experiment drastically increased the signal that reached the detector and enabled us to perform much improved studies.

After being diffracted by the analyzer, the beam was refocused into a germanium detector positioned directly above the scatterer as shown in Figure 4. A piece of lead tape was placed around the front beryllium window to minimize unwanted scattering background. Inside of the detector, the x-ray beam interacted with semi-conducting Ge diodes sensitive to the ionizing radiation. As a result, electrons were knocked out of the semi-conducting material. Finally, the electrons were drawn to an anode similar to the one in the ionizing chamber. A pulse proportional to the energy of the photons was produced, and a ~400 eV discriminator window around the wanted energy provided an additional background removal. The detector was then operated in photon-counting mode.

RESULTS

In Experiment I, a spreadsheet comparing the horizontal distance between the analyzer and laser and the vertical size of the diffracted beam just below the laser was created for each of the eight analyzers tested. Measurements of the diffracted beam were taken at distance intervals of 2.54 mm along the region containing the smallest focal size. Farther away from the focus, multiples of this distance were utilized for their efficiency at covering space as well as for their structural reinforcement in the graphs that were to be created later (see Table 1 and Figure 2). Although the smallest focal sizes were easily identified with the numbers collected, graphs were made so that the minimum regions could be examined in greater detail. Points along these regions were then scaled to a larger size so that a smooth best-fit curve could be drawn in by hand. This method allowed for the focal distances to be even more accurately depicted (see Figure 2). A chart containing both the manufacturers' quoted and experimentally determined focal lengths is shown in Table 2.

Our measured values for the focal lengths were then used by us in Experiment II where the energy resolution of the analyzers was studied. This was done by scanning the incident x-ray energy through the energy range of the analyzer. We then obtained the total energy resolution which is the convolution of both monochromator and analyzer resolutions. The graphs produced by the detector (see Figure 6) relating the energy of the incident beam and the intensity of the photons reaching the detector were used to determine these resolutions using Full Width Half Maximum (FWHM). This method found the total energy resolution of the system by the measured width of the line at half the vertical height of the curve.

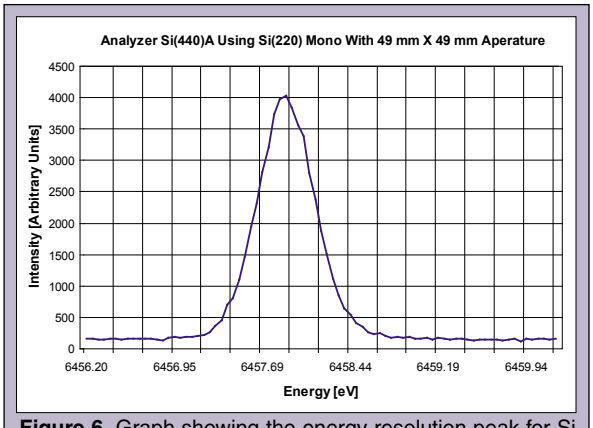

Figure 6. Graph showing the energy resolution peak for Si (440)A which, overall, had the best resolution.

Distance from Laser to Front Edge of Analyzer [mm]	Reading From Telescope	Size of Reflected Beam [mm]
1058.19	NA	5.00
1050.60	NA	4.00
1043.01	120.00	3.05
1035.42	100.00	2.54
1030.36	89.00	2.26
1027.83	80.00	2.03
1025.30	71.00	1.80
1022.77	66.00	1.68
1020.24	50.00	1.27
1017.71	31.00	0.79
1015.18	22.00	0.56
1012.65	22.00	0.56
1010.12	32.00	0.81
1007.59	50.00	1.27
1005.06	80.00	2.03
1002.53	100.00	2.54
1000.00	NA	3.00
997.47	NA	3.50
992.41	NA	4.00
987.35	NA	4.75
982.29	NA	6.00
977.23	NA	6.50

Table 1. Example spreadsheet relating distance to size of focus for Si(440)A.

Assuming that the resolution profiles were of Gaussian shape, the total resolution ΔE_{TOT} is given by the formula

$$\Delta E_{TOT} = (\Delta E_{MONO}{}^2 + \Delta E_{ANAL}{}^2)^{1/2} \qquad (4)$$

where ΔE_{ANAL} refers to the analyzer resolution and ΔE_{MONO} to the monochromator resolution. Using a theoretical value for ΔE_{MONO} of 0.40 eV, we then solved Eq. 4 for the analyzer energy resolution ΔE_{ANAL}. Since this value for ΔE_{MONO} describes the best possible monochomator resolution, our derived values for ΔE_{ANAL} are the worst case scenario and likely to be somewhat better. The experiment employed the analyzers of 90-100 mm diameter being tested fully exposed to the scattered radiation. Soon after, more readings were taken with an aperture of lead tape containing a 49 mm X 49 mm cutout being centered over the front of the analyzer. Table 3 and Table 4 were recorded.

DISCUSSION AND CONCLUSION

Overall, the eight analyzers performed similarly. Each of the eight analyzers tested was concluded to have a focal length within 3 cm of what was suggested by the manufacturer. Furthermore, seven of the eight were within 1.52 cm of those figures (see Table 2). We speculate that most of the focal lengths being slightly longer than what was quoted by the manufacturer was a result of less stress in the center regions of the Si and Ge wafers after being mounted to the glass substrates via glue or ionic bonding. Very slight bumps behind the wafers as some were mounted with glue may have been potential causes of imperfect energy resolutions.

Analyzer	Manufacturer's Quote Focal Length [mm]	Experimental Focal Length [mm]
Si(111)A	850	861.2
Si(111)B	1000	1015.2
Ge(111)C	850	860.2
Si(440)A	1000	1015.2
Si(440)B	1000	971.8
Si(440)C	850	848.5
Si(440)D	850	860.2
Ge(440)E	1000	1002.1

Table 2. Chart with results from Experiment I comparing experimentally determined focal lengths to manufacturers' quote focal lengths.

Si (440)A was found to have the best resolution at an energy range around 6.46 keV (See Tables 3 and 4). Its resolution increased by about a factor of two after the lead aperture was positioned over it to hide more than 2/3 the original surface area of the crystal wafer. It performed the best in 4 of 5 experiments done using 4 different Si(440) samples. Our speculations are that Si(440)A gave the best resolution because it used a slightly thicker silicon wafer (0.50 mm) and ionic bonding as compared to glue for the other three tested for resolution.

The usefulness of the experiments in accomplishing resolution in the new X-ray Raman spectrometer to be assembled at a later date was quite evidenced. Soon after the Si (440)A sample was determined to have the best energy resolution, the sample was used to prealign a goniometer for 7 analyzers into a Rowland geometry. Meanwhile, the orders for the analyzers of model Si (440)A were placed. Future projects include the assembly of the complete spectrometer employing 28 such analyzers, and testing of more

Using Si(220) Beamline Monochromator, 0.12 mm X 1.0 mm Beam Size, Full Analyzer Exposure	Si(440)A	Si(440)B	Si(440)C	Si(440)D
Diameter [mm]	100	100	100	90
Experimental Focal Length [mm]	1015.2	971.8	848.5	860.2
Total Resolution FWHM [eV] Beam Energy [eV]	0.91 6457.9	1.0 6458.5	1.1 6458.5	0.87 6458.7
Analyzer Resolution Assuming Mono Res = 0.40eV	0.82	0.92	1.02	0.88

Table 3. Chart with results from Experiment II. The total resolution was recorded in the detector, the monochromator resolution was given, and the analyzer resolution was derived from the two using Eq. 4.

Using Si(220) Beamline Monochromator, 0.12 mm X 1.0 mm Beam Size, 49 mm X 49 mm Aperture	Si(440)A	Si(440)B	Si(440)C	Si(440)D
Diameter [mm]	100	100	100	90
Experimental Focal Length [mm]	1015.2	971.8	848.5	860.2
Total Resolution FWHM [eV] Beam Energy [eV]	0.56 6457.9	0.59 6458.5	0.61 6458.9	0.64 6458.9
Analyzer Resolution Assuming Mono Res = 0.40eV	0.39	0.43	0.46	0.50

Table 4. Chart with second set of results from Experiment II. An aperture was used to limit the exposure of the analyzer.

analyzers at different energies. This instrument is expected to be the most efficient of its kind world wide.

ACKNOWLEDGEMENTS

I would like to thank the U. S. Department of Energy for providing me the opportunity to participate in the SULI summer internship program at Stanford Linear Accelerator Center and for giving me the chance to experience such an intellectually-stimulating research environment. A special thanks goes to my mentor, U. Bergmann, a noteworthy researcher and scientist for whom I have developed great respect. Thank you again for all the knowledge you were willing to share. I would also like to thank Mike Toney and Apurva Mehta for starting me out on the project. Greetings go out to A. Pierce.

REFERENCES

[1] Castelvecchi, Davide. "Favorite Liquid Revisited," SLAC Press Release, April 2004 <http://www.slac.stanford.edu/slac/media-info/20040402/>.

[2] Wernet, Ph; Nordlund, D; Bergmann, U; Ogasawara, H; Cavalleri, M; Näslund, LÅ; Hirsch, TK; Ojamäe, L; Glatzel, P; Odelius, M; Pettersson, LGM; & Nilsson, A. "The Structure of the First Coordination Shell in Liquid Water," Science, vol. 304, 2004, pp. 995.

[3] Bergmann, U; Wernet, Ph; Glatzel, P; Cavalleri, M; Pettersson, LGM; Nilsson, A; Cramer; SP. "X-ray Raman Spectroscopy at the Oxygen K-edge of Water and Ice: Implications on Local Structure Models." Phys. Rev. B, vol. 66, 092107, 2002.

[4] Bergmann, U. & Cramer, S.P. "A High-Resolution Large-Acceptance Analyzer for X-ray Fluorescence and Raman Spectroscopy," SPIE-Proceedings, vol. 3448, July 1998, pp. 198-209.

[5] Goodhew, Peter. "Diffraction," Matter Universities, July 2000 <http:// www.matter.org.uk/diffraction/>.

[6] Eric Gullikson. "X-ray Interactions With Matter: X-ray Transmission of a Gas," Center for X-ray Optics at Lawrence Berkeley Labs, 2004 <http://www. cxro.lbl.gov/optical_constants/gastrn2.html>.